Feedback Decoupling of Magnetically Coupled Actuators

M. Mohammadzadeh, M. R. Shariatmadari, N. Riahi, and A. Komaee

Abstract—Permanent magnet manipulators provide a unique potential for safe operation of magnetically driven medical tools inside the human body for noninvasive surgical, imaging, and drug targeting procedures. These systems manipulate magnetic objects from a distance without direct contact, by generating a magnetic f eld using strong permanent magnets, and controlling the shape of this feld properly. Control over the magnetic feld is gained by displacement of the magnets using independent mechanical actuators for each magnet. However, interactions between the magnets result in a coupling between the actuators, which prevents them from independent and precise operation. This paper develops a multivariate, nonlinear feedback control to cancel the magnetic coupling between the actuators in effect. This feedback control incorporates a complex mathematical model of the magnetic interactions between the actuators, which does not admit a simple analytical form. Instead, this model is constructed numerically using the finite element method. The decoupling performance of the proposed feedback control is verifed by numerical simulations.

I. INTRODUCTION

In a series of recent publications [1]–[5], we presented the concept of noncontact manipulation of magnetic objects by means of controllable arrays of permanent magnets. Multiple magnets in such arrays generate a magnetic feld and control its shape f exibly in order to apply magnetic forces of desired magnitude and direction to magnetic objects inside the feld. The shape of magnetic feld is controlled by displacement of the permanent magnets using mechanical actuators allocated to each magnet, which intend to control the position of their magnets independently. In practice, however, the actuators are coupled magnetically because of the interactions between their magnets. This coupling noticeably changes the dynamic and steady-state behavior of the actuators, and prevents them from operating independently. This paper aims to develop a multivariate feedback control technique to effectively cancel the magnetic coupling between the actuators.

Noncontact magnetic manipulators, consisting of arrays of mechanically adjustable permanent magnets or spatially f xed arrangements of electromagnets, have found a wide spectrum of medical [6]–[18] and microrobotics [19]–[23] applications which require to operate miniaturized tools from a distance without a direct mechanical contact. For instance, they can be utilized for operation of magnetically driven medical tools inside the human body for noninvasive surgical, imaging, and drug targeting procedures [6]–[18]. For medical applications, which typically require large magnetic forces at far distances

This work was supported by the National Science Foundation under Grant ECCS-1941944.

The authors are with the School of Electrical, Computer, and Biomedical Engineering, Southern Illinois University, Carbondale, IL 62901, USA email: akomaee@siu.edu.

of up to several decimeters, permanent magnets are preferred over electromagnets (if they are not the only feasible choice), as the magnetic f elds generated by electromagnets are much weaker than permanent magnets of similar size, weight, and cost [24].

Application of feedback control to magnetic manipulators enables them to accurately drive magnetic objects in desired directions at desired speeds, for instance, to precisely track a reference trajectory. In our previous work, we have proposed several control design approaches [2]–[5], [25]–[27] for both permanent magnet and electromagnet manipulators. Among our proposed approaches, the best performance is attained by a feedback linearization technique requiring the mechanical actuators to operate independently, precisely, and much faster than the dynamics of the magnetic object under control. Yet, all these requirements are violated by the inherent magnetic coupling between the actuators.

The remedy proposed in this paper is the application of an inner feedback loop to compensate for the magnetic coupling before applying the main feedback control via an outer loop. This inner feedback loop is a highly nonlinear, multivariate state feedback designed based on a mathematical model for the magnetic interactions between the actuators. This model is highly complex and does not admit a tractable analytical form; instead, it must be constructed numerically using the finite element method.

Section II describes the coupled dynamics of the actuators by a state-space model, which is employed then to develop a decoupling state feedback. This control is later enhanced by a mild integral action to ensure zero steady-state error without seriously altering the dynamics of actuators, optimized by the manufacturer. The state-space model of Section II includes a highly nonlinear function representing the magnetic coupling between the actuators. This function is numerically obtained in Section III using a f nite element software. In Section IV, the decoupling performance of feedback control is evaluated by numerical simulations.

II. DECOUPLING FEEDBACK CONTROL

This paper aims to develop a general method for feedback decoupling of magnetically coupled actuators applicable to a variety of magnetic manipulators. For demonstration of this method, the planar magnetic manipulator of Fig. 1 is adopted, which we first introduced in [5]. As shown schematically in Fig. 1(a), this manipulator consists of a circular array of six diametrically magnetized cylindrical permanent magnets, each equipped with a servomotor which can freely rotate it a full 360°. By controlling the directions of all six magnets, the total magnetic field generated by the array can be controlled,

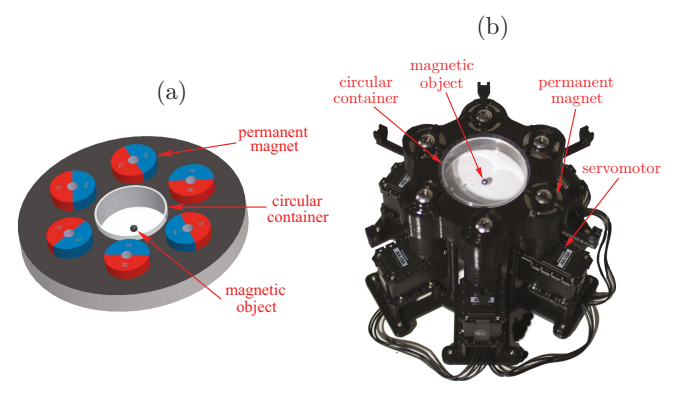


Fig. 1. Planar magnetic manipulator with a circular array of six rotatable, diametrically magnetized permanent magnets: (a) schematic diagram; (b) experimental setup. The permanent magnets can freely rotate a full 360° inside their guiding cylinders using 6 independent servomotors.

which is then exploited to control the motion of magnetic objects inside this magnetic feld [1]-[5].

After developing our f rst prototype shown in Fig. 1(b), it turned out that the interaction between the magnets was more severe than expected. Therefore, feedback decoupling of the actuators is necessary for accurate operation of the magnetic manipulator. Based on a nonlinear state-space model of the coupled servomotors developed in Section II-A, a decoupling feedback control is presented in Section II-B.

A. Dynamical Model of Magnetically Coupled Servomotors

Each servomotor in the magnetic manipulator of Fig. 1(b) is a coreless DC motor with an internal feedback loop aimed to adjust its angular position according to a reference input, rapidly and precisely. This built-in feedback utilizes a sensing device to measure the angular position of the DC motor, and effectively controls the motor to adjust the measured value as required by the reference input (the desired angular position). The second order linear dynamics [28] of the servomotor is represented by the transfer function

$$H(s) = \frac{\omega_n^2}{s^2 + 2\zeta\omega_n s + \omega_n^2} \tag{1}$$

from the reference input to the actual angular position of the servomotor. We experimentally verified this transfer function by recording the step response of the individual servomotors, as shown in Fig. 2. According to this f gure, the step response of the transfer function (1) closely f ts the empirical data with the parameters $\zeta=0.75$ and $\omega_n=75$ rad/sec.

Let $u_k(t)$ and $\theta_k(t)$ be respectively the input and output angles of servomotor $k=1,2,\ldots,6$ with respect to a fixed reference direction. Further, assume that $\tau_k(t)$ is the torque applied to the servomotor k externally, in case of this paper, by other magnets. Denote by $\Theta_k(s)$, $U_k(s)$, and $T_k(s)$, the Laplace transforms of $\theta_k(t)$, $u_k(t)$, and $\tau_k(t)$, respectively. Then, the angular position of the servomotor k is given by

$$\Theta_k(s) = \frac{\omega_n^2}{s^2 + 2\zeta\omega_n s + \omega_n^2} (U_k(s) - k_L T_k(s)),$$

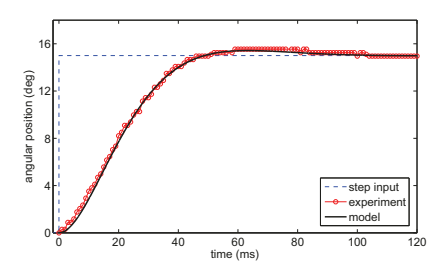


Fig. 2. Step response of the servomotors used in the experimental setup of Fig. 1(b) obtained experimentally (markers), and generated from the second order transfer function (1) (solid line) with the parameters $\omega_n=75$ rad/sec and $\zeta=0.75$. The experiment was performed in the absence of magnetic coupling but the servomotor was loaded by its own magnet.

where $k_L > 0$ is a constant. This input-output representation can be equivalently expressed as the state-space equations

$$\dot{\theta}_{k}(t) = \omega_{k}(t)$$

$$\dot{\omega}_{k}(t) = -2\zeta \omega_{n} \omega_{k}(t) - \omega_{n}^{2} \theta_{k}(t) + \omega_{n}^{2} u_{k}(t) - \omega_{n}^{2} k_{L} \tau_{k}(t)$$

by taking the angular velocity $\omega_k(t)$ as a state variable.

In the magnetic manipulator of Fig. 1, the external torque applied to servomotor k is caused by interactions between the permanent magnets and is a function of the angular positions of all servomotors, that is

$$\tau_k(t) = \tau_k(\theta_1(t), \theta_2(t), \theta_3(t), \theta_4(t), \theta_5(t), \theta_6(t)).$$
 (2)

The dependence of $\tau_k(t)$ on all angles $\theta_i(t)$, $i=1,2,\ldots,6$ results in the coupling of the dynamics of all 6 servomotors. This dynamics is then expressed in the vector form using the state-space equations

$$\dot{\theta}(t) = \omega(t)$$

$$\dot{\omega}(t) = -2\zeta\omega_n\omega(t) - \omega_n^2\theta(t) + \omega_n^2u(t) - \omega_n^2k_L\tau(\theta(t)),$$

where $\theta(t)$, $\omega(t)$, and u(t) are 6×1 vectors consisting of all the output angles $\theta_k(t)$, angular velocities $\omega_k(t)$, and input angles $u_k(t)$, respectively. Correspondingly, $\tau(\cdot): \mathbb{R}^6 \to \mathbb{R}^6$ is a vector function containing all 6 scalar functions (2). The construction of this vector function is detailed in Section III.

By applying a constant input vector u_{ss} to the system of 6 coupled servomotors, the steady-state output vector θ_{ss} of the system solves the algebraic equation $u_{ss} - \theta_{ss} = k_L \tau \left(\theta_{ss}\right)$, which indicates that $k_L \tau \left(\theta_{ss}\right)$ is the steady-state error caused by magnetic coupling under the input u_{ss} . Then, the largest possible error in each servomotor is given by

$$\varepsilon = \max_{\theta \in [0, 2\pi]^6} k_L \| \tau (\theta) \|_{\infty}.$$

Then, by defining the vector function

$$f\left(\theta\right) = \frac{\tau\left(\theta\right)}{\max_{\theta' \in [0,2\pi]^{6}} \left\|\tau\left(\theta'\right)\right\|_{\infty}},$$

the overall dynamics of the system of 6 magnetically coupled servomotors is expressed in the more intuitive form

$$\dot{\theta}(t) = \omega(t) \tag{3a}$$

$$\dot{\omega}(t) = -2\zeta\omega_n\omega(t) - \omega_n^2\theta(t) + \omega_n^2u(t) - \omega_n^2\varepsilon f(\theta(t)).$$

(3b)

Experiments performed on the setup of Fig. 1(b) indicate that its maximum angular error is around $\varepsilon=4^\circ$ [29], which is substantially larger than the unloaded resolution 0.3° of the individual servomotors. The goal of feedback control shortly introduced is to restore the precision of the servomotors and cancel the effect of magnetic coupling between them.

B. Controller Design

The structure of the state-space equations (3) suggests the simple state feedback law

$$u(t) = \theta_r(t) + \varepsilon f(\theta(t)) \tag{4}$$

to compensate for the magnetic coupling of the servomotors. Here, $\theta_r(t)$ is the 6×1 vector of new reference inputs to the servomotors after compensation. Application of the feedback control (4) to the state-space equations (3) results in the fully decoupled dynamics

$$\dot{\theta}(t) = \omega(t)$$

$$\dot{\omega}(t) = -2\zeta\omega_n\omega(t) - \omega_n^2\theta(t) + \omega_n^2\theta_r(t)$$

for the servomotors.

The major obstacle to this approach is that computation of the vector-valued function $f(\cdot)$ is not feasible in real time, as discussed in Section III. The obvious remedy is to modify the state feedback (4) as

$$u(t) = \theta_r(t) + \varepsilon \tilde{f}(\theta(t))$$
 (5)

with the best possible approximation $\tilde{f}(\cdot)$ for $f(\cdot)$, which is suitable for real-time implementation. The main contribution of this paper is the development of such approximate $\tilde{f}(\cdot)$, as is detailed in Section III.

Under the feedback control (5), the magnetic coupling of the servomotors is mostly but not completely compensated, as indicated by the closed-loop dynamics

$$\begin{split} \dot{\theta}\left(t\right) &= \omega\left(t\right) \\ \dot{\omega}\left(t\right) &= -2\zeta\omega_{n}\omega\left(t\right) - \omega_{n}^{2}\theta\left(t\right) + \omega_{n}^{2}\theta_{r}\left(t\right) - \omega_{n}^{2}\varepsilon\delta f\left(\theta\left(t\right)\right). \end{split}$$

Here, $\delta f\left(\cdot\right)=f\left(\cdot\right)-\tilde{f}\left(\cdot\right)$ is the approximation error, which is supposed to have a maximum value

$$\eta = \max_{\theta \in [0, 2\pi]^6} \left\| f(\theta) - \tilde{f}(\theta) \right\|_{\infty}$$

much smaller than 1. Then, the feedback control (5) reduces the maximum steady-state error by a factor of η .

To compensate for the remaining small steady-state error, the feedback control (5) can be enhanced by a mild integral action according to

$$\dot{q}(t) = \theta_r(t) - \theta(t) \tag{6a}$$

$$u(t) = \theta_r(t) + \varepsilon \tilde{f}(\theta(t)) + \omega_n k_I q(t). \tag{6b}$$

The integral gain $k_I > 0$ is chosen large enough to effectively compensate for the steady-state error, and small enough to not severely alter the dynamics of servomotors optimized by their manufacturer. The block diagram of Fig. 3 characterizes

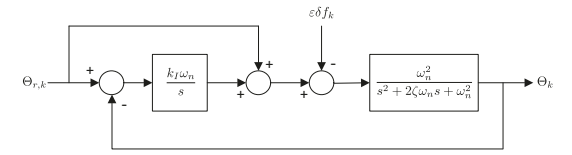


Fig. 3. Block diagram of each individual servomotor compensated with an integral controller.

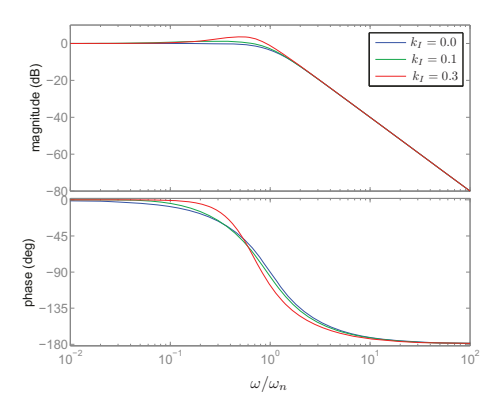


Fig. 4. Frequency response of servomotors under the integral control with different gains.

each individual servomotor under the integral compensation. The transfer function of this black diagram is given by

$$H_I(s) = \frac{(s/\omega_n) + k_I}{(s/\omega_n)^3 + 2\zeta (s/\omega_n)^2 + (s/\omega_n) + k_I}$$

from the scalar input $\theta_{r,k}(t)$ to the scalar output $\theta_k(t)$. The frequency response of this linear system is shown in Fig. 4 for the values $k_I=0,0.1,0.3$. According to this f gure, an integral gain $k_I<0.1$ is a suitable choice, as it only slightly modif es the dynamics of individual servomotors.

To simplify the feedback control (6), it might be tempting to drop the nonlinear compensation term $\varepsilon \tilde{f}\left(\theta\left(t\right)\right)$ from the right-hand side of (6b) and try to decouple the servomotors simply by a sole integral action. However, this approach often requires a larger integral gain, which can substantially change the optimized dynamics of the servomotors, and even more crucially, can lead to instability due to the highly nonlinear nature of the magnetic coupling $\varepsilon f\left(\theta\left(t\right)\right)$ in (3).

III. MODELING OF MAGNETIC INTERACTIONS

Implementation of the ideal state feedback (4) requires to compute the vector-valued function $f(\cdot)$ in real time. Since the complex structure of this function does not admit a simple analytical form, it can be only computed numerically using a finite element software such as COMSOL Multiphysics. The procedure for numerical construction of $f(\cdot)$ begins with the construction of a COMSOL model describing the geometry and material properties of the experimental setup of Fig. 1(b), as shown partly in Fig. 5. Based on this model, COMSOL generates a MATLAB function to compute the torque applied to each magnet for any given instance of the vector θ . This function can be directly called by MATLAB for the purpose of simulations or any other use.

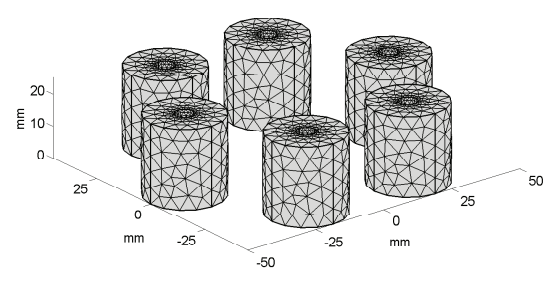


Fig. 5. Part of the COMSOL model developed for the magnetic manipulator of Fig. 1(b). Using this model, COMSOL computes the total torque applied to each magnet from all other magnets.

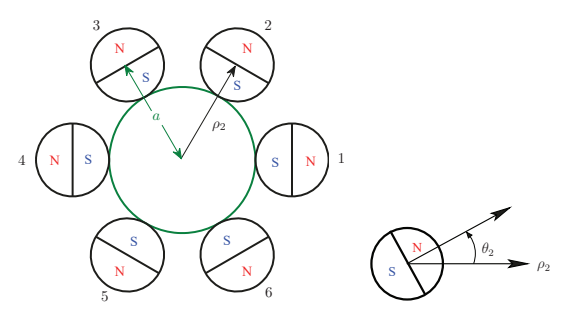


Fig. 6. Equidistant arrangement of 6 cylindrical magnets around a circular region and the coordinate systems for measuring their angular positions. The distance between the center of circular region and the center of each magnet is a. The angular position of each magnet is measured counterclockwise between its line of sight ρ_k to the center and its north pole direction.

This MATLAB function is computationally expensive and its runtime is far larger than a typical sampling time required for implementation of the state feedback (4). This runtime is certainly affordable for the simulations of Section IV, but is not suitable for real-time implementation. An alternative for real-time implementation, apparently, is the use of a lookup table constructed non-real-time. Yet, this method is infeasible for a function of 6 variables. To achieve a resolution of 0.3° comparable to that of the servomotors, the lookup table must have $(360/0.3)^6 \sim 3 \times 10^{18}$ elements.

In the remainder of this section, an approximation $\tilde{f}(\cdot)$ for the exact function $f(\cdot)$ is proposed which is feasible for real-time implementation by means of a lookup table. To explain the construction of this approximate function, the coordinate systems used for defining the angular positions $\theta_1, \theta_2, \ldots, \theta_6$ are shown in Fig. 6. This f gure illustrates a circular array of 6 cylindrical magnets numbered from 1 to 6 counterclockwise. The distance between the center of the circular array and the center of each magnet is denoted by a. The angular position of each magnet is measured counterclockwise from its line of sight to the center of array toward the direction of its north pole, and is denoted by θ_k for magnet k.

The approximate function $\tilde{f}(\cdot)$ is determined based on the following guidelines. First, the torque applied to each magnet from 5 other magnets is characterized by the superposition of the pairwise interactions between this magnet and 5 others. Second, only the interactions between adjacent magnets are counted, as these interactions rapidly weaken with distance. Specif cally, let $\tau_{i \to j} \left(\theta_i, \theta_j \right)$ denote the torque applied from magnet i to magnet j in the absence of other magnets. This

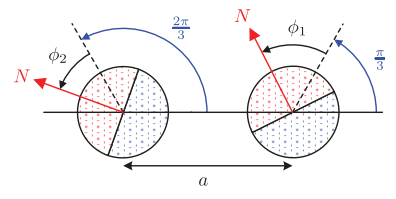


Fig. 7. Coordinate system for construction of pairwise interaction between a pair of magnets.

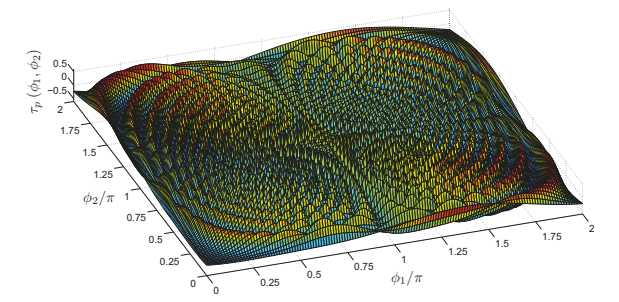


Fig. 8. Surface plot of the pairwise torque τ_p (ϕ_1, ϕ_2) measured in N·m.

function clearly holds the property

$$\tau_{j \to i} (\theta_j, \theta_i) = -\tau_{i \to j} (\theta_i, \theta_j).$$

Suppose $\tilde{\tau}(\theta)$ is a vector containing the approximate torques applied to all 6 magnets. Then, this vector is represented by

$$\tilde{\tau}(\theta) = \begin{bmatrix} \tau_{6\to 1} (\theta_6, \theta_1) - \tau_{1\to 2} (\theta_1, \theta_2) \\ \tau_{1\to 2} (\theta_1, \theta_2) - \tau_{2\to 3} (\theta_2, \theta_3) \\ \tau_{2\to 3} (\theta_2, \theta_3) - \tau_{3\to 4} (\theta_3, \theta_4) \\ \tau_{3\to 4} (\theta_3, \theta_4) - \tau_{4\to 5} (\theta_4, \theta_5) \\ \tau_{4\to 5} (\theta_4, \theta_5) - \tau_{5\to 6} (\theta_5, \theta_6) \\ \tau_{5\to 6} (\theta_5, \theta_6) - \tau_{6\to 1} (\theta_6, \theta_1) \end{bmatrix}.$$
(7)

The specif c definition of the angles $\theta_1,\theta_2,\ldots\theta_6$ in Fig. 6 makes it possible to express all functions $\tau_{i\to j}$ (·) in (7) as a single function τ_p (ϕ_1,ϕ_2) describing the pairwise interaction of two adjacent magnets. By defining the angles ϕ_1 and ϕ_2 as shown in Fig. 7, the magnetic torque applied from the magnet on the right-hand side of the f gure to the magnet on the left is denoted by the bivariate function τ_p (ϕ_1,ϕ_2). This function is numerically constructed by COMSOL, as shown in Fig. 8.

In terms of τ_p (ϕ_1 , ϕ_2), the approximate vector function (7) can be expressed as

$$\tilde{\tau}(\theta) = \begin{bmatrix} -1 & 0 & 0 & 0 & 0 & 1\\ 1 & -1 & 0 & 0 & 0 & 0\\ 0 & 1 & -1 & 0 & 0 & 0\\ 0 & 0 & 1 & -1 & 0 & 0\\ 0 & 0 & 0 & 1 & -1 & 0\\ 0 & 0 & 0 & 0 & 1 & -1 \end{bmatrix} \begin{bmatrix} \tau_p(\theta_1, \theta_2)\\ \tau_p(\theta_2, \theta_3)\\ \tau_p(\theta_3, \theta_4)\\ \tau_p(\theta_3, \theta_4)\\ \tau_p(\theta_4, \theta_5)\\ \tau_p(\theta_5, \theta_6)\\ \tau_p(\theta_6, \theta_1) \end{bmatrix}.$$
(8)

This function is normalized next to determine

$$\tilde{f}(\theta) = \frac{\tilde{\tau}(\theta)}{\max_{\theta' \in [0,2\pi]^6} \|\tau(\theta')\|_{\infty}}$$

as an approximation for $f(\cdot)$.

For real-time computation of the approximation $\tilde{f}(\cdot)$, the bivariate function $\tau_p(\phi_1, \phi_2)$ can be tabulated with sufficient

resolution. For a resolution of 0.3° , this function is expressed by $(360/0.3)^2 = 1.44 \times 10^6$ elements. If each element of the table is represented by 16 bytes, the total memory needed for its storage will be 23 megabytes, which is affordable by any modern computer. Application of lookup tables in modeling pairwise interactions between actuators is not limited to the specific magnetic manipulator of this paper and is extendable to magnetic manipulators of diverse designs and geometries.

For the magnetic manipulator of this paper, in particular, an approach more efficient than lookup table can be adopted. Since τ_p (ϕ_1, ϕ_2) is periodic with respect to both ϕ_1 and ϕ_2 , it can be represented by a bivariate Fourier series. This series certainly has inf nite number of terms for exact representation of τ_p (ϕ_1, ϕ_2); however, an arbitrarily close approximation is achievable using a finite but large enough number of terms. This approximation is expressed as

$$\tau_p(\phi_1, \phi_2) \simeq \sum_{i=1}^{N} \sum_{j=1}^{N} a_{ij} \cos(i\phi_1 + j\phi_2 + \psi_{ij})$$

with a sufficiently large N and the parameters a_{ij} and ψ_{ij} extracted from the numerical values of τ_p (ϕ_1, ϕ_2) generated by COMSOL.

IV. SIMULATION RESULTS

Computer simulations have been performed to evaluate the decoupling performance of the proposed feedback controls. Some results of this study are presented in this section under the following scenario. The reference positions of all magnets but magnet 1 are kept f xed at 0° during the experiment, and for this single magnet, the reference is abruptly changed from the initial value 0° to the f nal value 30° . For this test signal, the step response of servomotor 1 is obtained in the presence of magnetic coupling with other magnets. This step response is generated for three scenarios: without feedback decoupling of the servomotors, with feedback decoupling under the state feedback (5), and with feedback decoupling enhanced by the integral action according to (6).

The parameter values used for the simulations have been determined as $\zeta=0.75$ and $\varepsilon=0.07$ rad via experiments performed on the servomotors and the setup of Fig. 1(b). The simulation results are presented for the normalized time $\omega_n t$ and normalized angular velocity $\omega(t)/\omega_n$, so the normalized value $\omega_n=1$ was adopted for numerical simulations of the state-space equation (3). The integral action in the control (6) was implemented with the gain $k_I=0.002$.

The step response of servomotor 1 is illustrated in Fig. 9. As indicated by this f gure, the magnetic coupling results in a signif cant steady-state error, if left uncompensated. Further, it is observed that the magnetic coupling mostly introduces a steady-state error with only a slight change in the dynamical behavior of the servomotors. Fig. 9 indicates that both state feedback (5) and its integral enhanced upgrade (6) effectively cancel the magnetic coupling between the servomotors. Yet, the integral action noticeably improves the steady-state error, as shown in Fig. 10.

Fig. 11 presents a numerical comparison between the exact magnetic torque τ_1 (θ) applied to servomotor 1 and $\tilde{\tau}_1$ (θ), its

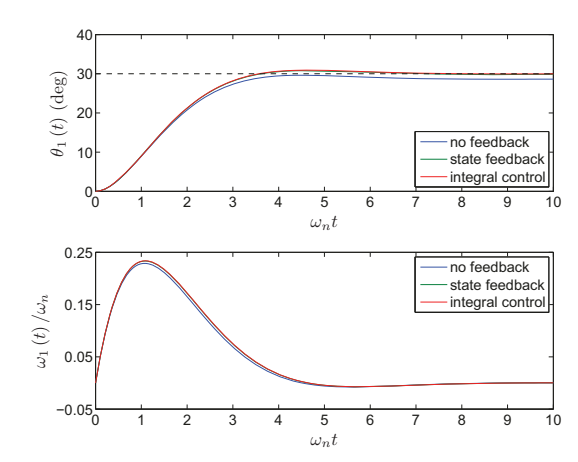


Fig. 9. Step response of servomotor 1 in the presence of magnetic coupling with other magnets, without decoupling control, under the state feedback (5), and under the integral controller (6). The step response under the state feedback is barley distinguished from that of the integral control.

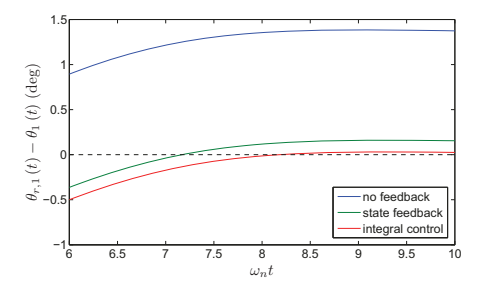


Fig. 10. Tracking error of servomotor 1, without decoupling control, under the state feedback (5), and under the integral control (6).

approximation (8). In this f gure, $\tau_1(\theta_1e_1)$ and $\tilde{\tau}_1(\theta_1e_1)$ are illustrated versus θ_1 , where $e_1=(1,0,0,0,0,0)$. The close match observed between the graphs of this f gure evidences the soundness of the approximation method of Section III.

V. CONCLUSION AND FUTURE WORK

Permanent magnet manipulators render a unique ability to actuate and control magnetic objects from a distance without direct mechanical contact, which is exploited for operation of magnetically driven medical tools inside the human body for noninvasive surgical, imaging, and drug targeting procedures. These systems utilize mechanical actuators to independently control the position of permanent magnets arranged in spatial arrays in order to generate a controllable magnetic feld used for noncontact manipulation of magnetized tools. Yet, the magnetic coupling between the actuators prevents them from independent and precise operation. To compensate for the magnetic coupling, a multivariate, nonlinear feedback control was developed based on a model of the interactions between the magnets. Due to the complex nature of this model, it was constructed numerically using a finite element software. The performance of the decoupling feedback control was verified by computer simulations.

Although the simulation results verify the effectiveness of feedback control in restoring the actuators dynamics, another severe consequence of magnetic coupling cannot be canceled by means of feedback. Strong magnetic coupling between the

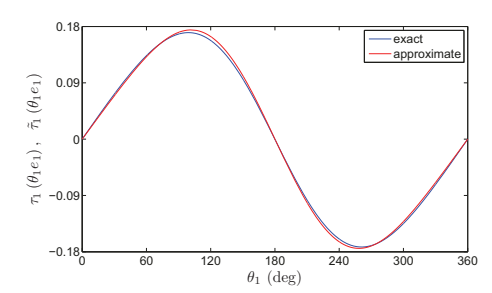


Fig. 11. Exact and approximate magnetic torque applied to servomotor 1 versus its angular position θ_1 , while other magnets are positioned at 0° .

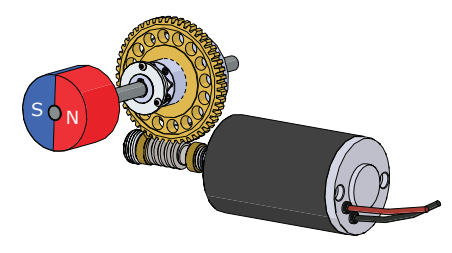


Fig. 12. Unidirectional transmission of torque from motor to magnet using a worm gear mechanism.

servomotors results in substantial stall current, which in turn, results in energy loss, overheating of the motors, and higher cost to utilize stronger motors. This difficulty can be rectifed by a worm gear mechanism for unidirectional transmission of torque from motors to magnets, as shown in Fig. 12. Detailed investigation of this modification is planned as future work.

REFERENCES

- N. Riahi and A. Komaee, "Geometry optimization of a noncontact magnetic manipulator with rotatable permanent magnets," in *Proc. of* 2020 IEEE/ASME International Conference on Advanced Intelligent Mechatronics (AIM 2020), p. 417, 2020.
- [2] N. Riahi and A. Komaee, "Noncontact steering of magnetic objects by optimal linear feedback control of permanent magnet manipulators," in Proc. of 2020 IEEE/ASME International Conference on Advanced Intelligent Mechatronics (AIM 2020), pp. 30–35, 2020.
- [3] N. Riahi, L. R. Tituaña, and A. Komaee, "Homotopy continuation for feedback linearization of noncontact magnetic manipulators," in *Proc.* of 2020 American Control Conference (ACC 2020), pp. 4295–4300, 2020.
- [4] N. Riahi and A. Komaee, "Noncontact direction control of magnetic objects by permanent magnet manipulators," in *Proc. of 2020 Ameri*can Control Conference (ACC 2020), p. 1080, 2020.
- [5] N. Riahi and A. Komaee, "Steering magnetic particles by feedback control of permanent magnet manipulators," in *Proc. of 2019 American Control Conference (ACC 2019)*, pp. 5432–5437, 2019.
- [6] M. Sendoh, K. Ishiyama, and K.-I. Arai, "Fabrication of magnetic actuator for use in a capsule endoscope," *IEEE Trans. Magn.*, vol. 39, no. 5, pp. 3232–3234, 2003.
- [7] G. Ciuti, P. Valdastri, A. Menciassi, and P. Dario, "Robotic magnetic steering and locomotion of capsule endoscope for diagnostic and surgical endoluminal procedures," *Robotica*, vol. 28, no. 2, pp. 199– 207, 2010.
- [8] M. Simi, P. Valdastri, C. Quaglia, A. Menciassi, and P. Dario, "Design, fabrication, and testing of a capsule with hybrid locomotion for gastrointestinal tract exploration," *IEEE/ASME Trans. Mechatronics*, vol. 15, no. 2, pp. 170–180, 2010.
- [9] A. Komaee and B. Shapiro, "Magnetic steering of a distributed ferrof uid spot towards a deep target with minimal spreading," in *Proc.* of the 50th IEEE Conference on Decision and Control (CDC 2011), pp. 7950–7955, 2011.

- [10] S. Yim and M. Sitti, "Design and rolling locomotion of a magnetically actuated soft capsule endoscope," *IEEE Trans. Robot.*, vol. 28, no. 1, pp. 183–194, 2012.
- [11] S. Yim and M. Sitti, "Shape-programmable soft capsule robots for semi-implantable drug delivery," *IEEE Trans. Robot.*, vol. 28, no. 5, pp. 1198–1202, 2012.
- [12] G.-S. Lien, C.-W. Liu, J.-A. Jiang, C.-L. Chuang, and M.-T. Teng, "Magnetic control system targeted for capsule endoscopic operations in the stomach—design, fabrication, and in vitro and ex vivo evaluations," *IEEE Trans. Biomed. Eng.*, vol. 59, no. 7, pp. 2068–2079, 2012.
- [13] A. Nacev, A. Komaee, A. Sarwar, R. Probst, S. H. Kim, M. Emmert-Buck, and B. Shapiro, "Towards control of magnetic fuids in patients: directing therapeutic nanoparticles to disease locations," *IEEE Control Syst. Mag.*, vol. 32, no. 3, pp. 32–74, 2012.
- [14] A. Komaee, R. Lee, A. Nacev, R. Probst, A. Sarwar, D. A. Depireux, K. J. Dormer, I. Rutel, and B. Shapiro, *Magnetic Nanoparticles: From Fabrication to Clinical Applications*, ch. Putting Therapeutic Nanoparticles Where They Need to Go by Magnet Systems Design and Control, pp. 419–448. CRC Press, 2012.
- [15] M. Beccani, C. Di Natali, L. J. Sliker, J. A. Schoen, M. E. Rentschler, and P. Valdastri, "Wireless tissue palpation for intraoperative detection of lumps in the soft tissue," *IEEE Trans. Biomed. Eng.*, vol. 61, no. 2, pp. 353–361, 2014.
- [16] V. Iacovacci, L. Ricotti, P. Dario, and A. Menciassi, "Design and development of a mechatronic system for noninvasive reflling of implantable artificial pancreas," *IEEE/ASME Trans. Mechatronics*, vol. 20, no. 3, pp. 1160–1169, 2015.
- [17] L. Sliker, G. Ciuti, M. Rentschler, and A. Menciassi, "Magnetically driven medical devices: a review," *Expert Review of Medical Devices*, vol. 12, no. 6, pp. 737–752, 2015.
- [18] A. Komaee, "Feedback control for transportation of magnetic fuids with minimal dispersion: A first step toward targeted magnetic drug delivery," *IEEE Trans. Control Syst. Technol.*, vol. 25, no. 1, pp. 129– 144, 2017.
- [19] C. Gosse and V. Croquette, "Magnetic tweezers: Micromanipulation and force measurement at the molecular level," *Biophysical Journal*, vol. 82, no. 6, pp. 3314–3329, 2002.
- [20] M. B. Khamesee, N. Kato, Y. Nomura, and T. Nakamura, "Design and control of a microrobotic system using magnetic levitation," *IEEE/ASME Trans. Mechatronics*, vol. 7, no. 1, pp. 1–14, 2002.
- [21] S. Schuerle, S. Erni, M. Flink, B. E. Kratochvil, and B. J. Nelson, "Three-dimensional magnetic manipulation of micro- and nanostructures for applications in life sciences," *IEEE Trans. Magn.*, vol. 49, no. 1, pp. 321–330, 2013.
- [22] H. Marino, C. Bergeles, and B. J. Nelson, "Robust electromagnetic control of microrobots under force and localization uncertainties," *IEEE Trans. Autom. Sci. Eng.*, vol. 11, no. 1, pp. 310–316, 2014.
- [23] L. Chen, A. Offenhäusser, and H.-J. Krause, "Magnetic tweezers with high permeability electromagnets for fast actuation of magnetic beads," *Review of Scientif c Instruments*, vol. 86, no. 4, p. 044701, 2015.
- [24] O. Baun and P. Blümler, "Permanent magnet system to guide superparamagnetic particles," *J MAGN MAGN MATER*, vol. 439, pp. 294– 304, 2017.
- [25] A. Komaee and B. Shapiro, "Steering a ferromagnetic particle by optimal magnetic feedback control," *IEEE Trans. Control Syst. Technol.*, vol. 20, no. 4, pp. 1011–1024, 2012.
- [26] R. Probst, J. Lin, A. Komaee, A. Nacev, Z. Cummins, and B. Shapiro, "Planar steering of a single ferrof uid drop by optimal minimum power dynamic feedback control of four electromagnets at a distance," *Journal of Magnetism and Magnetic Materials*, vol. 323, no. 7, pp. 885–896, 2011.
- [27] A. Komaee and B. Shapiro, "Steering a ferromagnetic particle by magnetic feedback control: Algorithm design and validation," in *Proc.* of 2010 American Control Conference (ACC 2010), pp. 6543–6548, 2010.
- [28] R. Isermann, Mechatronic Systems: Fundamentals. London; New York: Springer, 2005.
- [29] L. R. Tituana, "Implementation of a planar magnetic manipulator with rotatable permanent magnets," Master's thesis, Southern Illinois University, Carbondale, 2020.